Bone formation on carbon nanotube composite

Mrinal Bhattacharya,[1] Patcharaporn Wutticharoenmongkol-Thitiwongsawet,[2] Darryl T. Hamamoto,[3] Dongjin Lee,[4] Tianhong Cui,[4] Hari S. Prasad,[3] Mansur Ahmad[3]

[1]Department Bioproducts and Biosystems Engineering, University of Minnesota, Saint Paul, Minnesota
[2]Faculty of Science, Polymer Science Program, Prince of Songkla University, Songkhla, Thailand
[3]Department of Diagnostic and Biological Sciences, School of Dentistry, University of Minnesota, Minneapolis, Minnesota
[4]Department of Mechanical Engineering, University of Minnesota, Minneapolis, Minnesota

Received 30 April 2010; revised 16 July 2010; accepted 30 July 2010
Published online 26 October 2010 in Wiley Online Library (wileyonlinelibrary.com). DOI: 10.1002/jbm.a.32958

Abstract: The effects of a layer-by-layer assembled carbon nanotube composite (CNT-comp) on osteoblasts *in vitro* and bone tissue *in vivo* in rats were studied. The effects of CNT-comp on osteoblasts were compared against the effects by commercially pure titanium (cpTi) and tissue culture dishes. Cell proliferation on the CNT-comp and cpTi were similar. However, cell differentiation, measured by alkaline phosphatase activity and matrix mineralization, was better on the CNT-comp. When implanted in critical-sized rat calvarial defect, the CNT-comp permitted bone formation and bone repair without signs of rejection or inflammation. These data indicate that CNT-comp may be a promising substrate for use as a bone implant or as a scaffold for tissue engineering. J Biomed Mater Res Part A: 96A: 75–82, 2011.

Key Words: carbon nanotube, osteoblast, titanium, critical sized defect, mineralization

INTRODUCTION

Carbon nanotubes (CNTs) are a promising material as a substrate for tissue engineering or for use as an implant material. Composites of CNT, due to high electrical conductivity and physical strength,[1] can be used for prosthetic neural devices or as implantable scaffolds in bone-tissue engineering. Electrical stimulus through CNTs enhances bone healing.[2,3] CNT composites can be fabricated to match mechanical properties of bone.[4,5] Even though the properties are promising, currently CNTs are not widely used in biomedical applications due to uncertainty about its safety.[6–8]

CNTs can be single-walled (SWCNT) or multiwalled (MWCNT). Adverse effects of unrefined SWCNTs include accelerated oxidative stress, decreased cell viability, and altered cell morphology.[7,9] Other adverse effects of SWCNTs include induction of apoptosis and decrease of cellular adhesion.[10] Adverse effects of nonfunctionalized MWCNTs include the release of pro-inflammatory cytokine.[11] Intratracheal inhalation of CNT particles in mice and rats can cause pulmonary toxicity.[12,13] These adverse effects may be due to lack of purity and functionalization. Purified SWCNTs do not create short-term toxic effects on cardiac-muscle cells.[14] Chemically functionalized CNTs and their surface charges had a positive impact on neuronal growth.[15,16] CNT fibers of larger diameters and lower surface energies had positive effects on cell attachment and proliferation.[17] SWCNTs were superior than MWCNTs in allowing spreading of osteoblast-like cells.[18]

To reduce the toxicity, control the dispersion of free CNT particles, and duplicate the shape of the body part to be replaced, CNT particles can be coated with different substrates to form composite. Coating substrates include polymers,[19–21] hydroxyapatite,[22] or collagen.[23] An ideal implantable composite should induce tissue growth, and also have good mechanical properties. A composite with collagen may not have physical properties or a modulus of elasticity similar to that of bone. Hydroxyapaptite coating can be brittle, but this limitation can be reduced by incorporating polymers.[24] With a polymer coating, the modulus of CNT composites can be matched to that of bone.[4,25] The use of CNT-based biomaterials for bone tissue engineering is still in its infancy. In particular, the effects of CNT-polymer composites *in vivo* have not been adequately demonstrated. We therefore evaluated the response of osteoblast *in vitro* and tissue *in vivo* to a polymer coated single-walled CNT composite (CNT-comp).

Currently, titanium-based materials are the most common materials used in dental implants and for repairing bone defects. Although titanium-based materials are tissue compatible, their physical and mechanical properties are not similar to native bone. Ceramic-coated metallic implants that are currently used in various clinical applications have elastic moduli 10 times higher than those of most hard tissues.[26] Hence, using metallic materials to repair bone defects cause the bone to be insufficiently loaded. This process, known as stress-shielding, affects bone remodeling and healing, resulting in increased bone porosity or atrophy.[27,28] These disadvantages of current implant materials highlight the need for developing new materials, such as a composite of CNTs.

Correspondence to: M. Ahmad; e-mail: ahmad005@umn.edu

In this study, we report on the biocompatibility of chemically functionalized CNTs as a composite with polymers. We used these CNT-composites (CNT-comp) to test osteoblast proliferation and morphology, and osteoblast differentiation by measuring alkaline phosphatase (ALP) activity and matrix mineralization. These results were compared to osteoblast responses on commercially pure titanium (cpTi), which is a frequently used implant substrate, and to tissue culture (TC) dishes. Response of CNT to bone in non-critically sized defects has been shown to be favorable.[29,30] We therefore, in addition to the *in vitro* tests, conducted a *in vivo* bone-tissue compatibility study of CNT-comp in a critically sized defect in rat calvaria.

MATERIALS AND METHODS

Preparation of CNT-comp

SWCNTs (1–2 nm in diameter and 50 μm in length) were functionalized in a 3:1 mixture of concentrated sulfuric and nitric acid. The nanotube suspension was filtered using a membrane (0.22 μm pore size) under vacuum to remove soot, metallic particles, and shorter SWCNTs. Longer SWCNTs, aggregates and bundles were eliminated with the aid of ultrasonication and centrifugation. The final concentration of SWCNT in aqueous solution was 0.06 wt %. Polycaprolactone (PCL) sheets (0.6 mm thick) were cleaned with a mixture of isopropanol/water (1:1 volume) for an hour and then washed thoroughly with deionized water. Oxygen plasma (50 sccm O_2 flow rate, 50 W power) was applied to the PCL sheets for 1 min to negatively charge the surface. Two bilayers of positively charged polydimethyldiallylammonium (PDDA) and negatively charged polystyrene sulfonate (PSS) were deposited on the PCL sheets using layer-by-layer self-assembly to enhance the charge density. The concentrations of PDDA and PSS were 1.4 and 0.3 wt %, respectively, in 0.5*M* sodium chloride and the dipping time was 10 min for both polyelectrolyte solutions. Polyethyleneimine (PEI) and SWCNTs were deposited alternately to produce $[(PDDA/PSS)_2(PEI/SWCNT)_6]_{10}PEI$ on the PCL sheets. The PEI concentration was kept at 1 wt %, and dipping times were 10 and 15 min for PEI and SWCNT, respectively.

Hardness test

The CNT-comp samples were tested at 10 arbitrarily selected points using a NanoIndenter XP (MTS Nano Instruments Innovation Center, Oak Ridge, TN) to calculate the hardness and the modulus.[31] For nanoindentation tests on coating/substrate systems, a 10% rule of thumb is widely used, that is, the indentation depth must be less than 10% of the coating thickness if the properties of the composite are to be extracted without the data being influenced by the substrate (in this case PCL, which has a modulus of 300 MPa).

Commercially pure titanium

Commercially produced 22 mm diameter titanium disks (cpTi) were kindly provided by Dr. PanJian Li (DePuy, Warsaw, IN). The disks were processed by glass bead blasting in the same manner as clinical implants.

Human osteoblast cultures

Human fetal osteoblast 1.19 (hFOB) cells[32] were a gift from Dr. Thomas Spelsberg (Mayo Clinic, Rochester, MN). Cells were cultured in 100 mm dishes (Corning, Corning, NY) in αMEM media (Life Technologies, St. Louis, MO) and 5% bovine serum complex (Fetalplex, Gemini, Woodland, CA) at 34°C in the presence of 5% carbon dioxide. At confluence, cells were trypsinized using 0.5% trypsin-EDTA (Invitrogen, Grand Island, NY), counted using a Z1 Coulter Counter (Coulter Electronics, Hialeah, FL), and plated in six-well dishes (Corning) at 50,000 cells/well. The day of plating was considered day 0 of the experiment.

Scanning electron microscopy

Morphology, spread, and distribution of the hFOB cells on the substrates were examined by scanning electron microscopy (SEM). Cells on the disks were fixed with glutaraldehyde in cacodylate buffer and then treated with osmium tetroxide in cacodylate buffer. The cultures were dehydrated in sequential concentrations of ethanol. After critical point drying, cells were sputter-coated with 10 nm of gold/palladium before examining them with a JEOL JSM 6320FV field emission scanning microscope (JEOL USA, Peabody, MA). We did not perform SEM on the cells grown on the TC surfaces.

Cellular proliferation

hFOB cells were cultured for 8 days, and then the wells were washed twice to remove nonattached cells. The substrate disks were transferred to new wells to count only the cells attached to the disks. Cells on tissue culture dishes (TC) were positive controls. Attached cells were trypsinized using 0.5% trypsin-EDTA, and then counted with a Coulter Counter. Cell counts were adjusted to account for the difference in the surface area between the disks and that of the six-well TC dishes.

Alkaline phosphatase activity

On day 8 of culture, hFOB cells were lysed by scrapping in 500 μL of harvesting buffer per well (10 m*M* Tris Cl, 0.2% NP40, and 2 m*M* phenylmethylsulfonyl fluoride). The extracted solution was sonicated and centrifuged. A commercially available kit (Stanbio, Boerne, TX) was used to determine ALP activity of the supernatant. The optical density of the supernatant at 405 nm was measured with a spectrophotometer (AD340, Beckman Coulter, Fullerton, CA). The ALP activity was expressed as micromolar of pNP/min/mg of protein.

Calcium content

The calcium content of the hFOB cell layer was assayed at 4 weeks of culture. The cell cultures were incubated twice for 30 min in 5% trichloroacetic acid (TCA). Calcium content in the combined TCA washes was measured colorimetrically with a calcium kit (Stanbio).

Energy dispersive spectroscopy

At 4 weeks of culture, all the test material surfaces were completely covered with hFOB cells. Cells were fixed with

3% formaldehyde solution and dehydrated in a series of increasing concentrations of ethanol solutions. Dried specimens were coated with carbon. Calcium and phosphorus elements were mapped by SEM (JEOL 6500F), which was connected to an energy dispersive spectroscopy (EDS).

Animal surgical procedure

Adult, male, Sprague-Dawley rats (250 gm body weight, Harlan, Indianapolis, IN) were used in this study. All animal procedures were approved by the Institutional Animal Care and Use Committee at the University of Minnesota. Rats were anesthetized with an intramuscular injection of ketamine (75 mg/kg) with xylazine (10 mg/kg). The hair over the calvarium was shaved and cleaned. After the skin was incised, a full-thickness circular critically sized defect (diameter of 1 cm) was made in the calvarium using an electrical drill with a sterile round bur under irrigation with sterile normal saline to avoid damage to the bone. A critically sized defect will not completely heal with bone without any exogenous support.[33] A sterilized CNT-comp disk of 1 cm diameter was placed into the defect, the surgical site was irrigated with sterile normal saline, and the wound was closed in layers with resorbable sutures. In one group of rats, the surgical defect was prepared but no implant was placed. There were three rats in each treatment group. All rats were examined daily for signs of infection or discomfort for 6 weeks.

Histological study

Six weeks after implantation of the disks, rats were sacrificed by CO_2 asphyxiation. Block sections of the calvarium containing the disks were harvested from the surgical sites and fixed in 10% neutral buffered formalin. Specimens were then dehydrated for 9 days with a graded series of alcohols. Following dehydration, specimens were infiltrated with a light-curing embedding resin (Technovit 7200 VLC, Kulzer, Wehrheim, Germany) for 20 days with constant shaking at normal atmospheric pressure. The embedding resin was polymerized by light (450 nm) with the temperature of the specimens never exceeding 40°C. Tissue sections were then prepared by modifying the cutting/grinding method of Donath.[34,35] Each section was cut to a thickness of 150 μm on an EXAKT cutting/grinding system (EXAKT Technologies, Oklahoma City). Slides were then polished to a thickness of 45 μm using the EXAKT microgrinding system followed by alumina polishing paste. Tissue sections were stained with Stevenel's blue and Van Gieson's picro fuchsin.

RESULTS

The CNT-comp was developed using the layer-by-layer (LbL) technique. Surfaces were created by alternately exposing a substrate to a positively (PDDA or PEI) and negatively-charged molecules (PSS and SWNT). This step was repeated until the desired number of bilayers (anionic-cationic pairs) was achieved. By controlling the pH of the solution, concentration of polymer, the molecular weight of the polymer, and the time of deposition, the thickness of the depositing layer can be precisely controlled. The thickness of a single bilayer in this study was approximately 85 Å, as measured by a surface profiler and an ellipsometer. CNT-comp sheets were cut into disks (15 mm diameter) for experiments. The topmost PEI layer is ~40 Å thick, and the CNTs were visible on the SEM image (Fig. 1). There is no cluttering of CNTs, and individual nanotubes were randomly oriented.

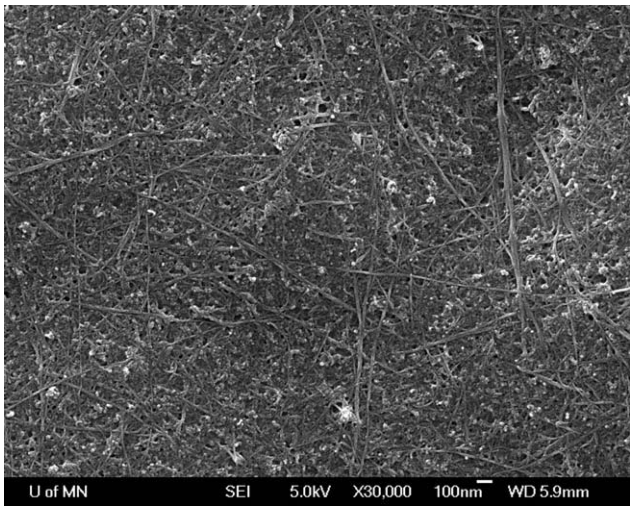

FIGURE 1. High magnification scanning electron micrograph of CNT-comp surface. Bar = 100 nm. The nanotubes are visible on the surface as crisscrossing linear structures. There is a layer of PEI coating the nanotubes.

A 10-layered CNT-comp sample ($[PDDA/PSS)_2(PEI/SWCNT)_6]_{10}PEI$) gave a lower hardness (0.1 ± 0.02 GPa) and modulus (2.5 ± 0.4 GPa) than cortical bone.[36,37] When the number was increased to 120 CNT-comp layers ($[PDDA/PSS)_2(PEI/SWCNT)_6]_{20}PEI$), the hardness (0.14 ± 0.05 GPa) and modulus (6.17 ± 2.40 GPa) increased. These results are consistent with those in the literature.[38] Several researchers[36,37,39,40] using similar technique have reported the modulus of trabecular and cortical bone to be of the same order of magnitude as the 120-layered CNT-composite. Also, these authors have reported that the nanoindented modulus and bulk modulus had similar values.

A successful tissue engineering substrate should promote cell attachment and proliferation. Scanning electron microscopy study showed that attachment and morphology of hFOB to CNT-comp and cpTi were time dependant. (Fig. 2) At 1 h after plating, osteoblasts on the substrates were round [Fig. 2(A,B)] At 24 h, cells had spread to assume roughly rectangular shape. Cells were wider on cpTi compared to those on CNT-comp [Fig. 2(C,D)], which can be attributed to the rougher cpTi surface.[41] At 72 h after plating, layered cells covered the surfaces [Fig. 2(E,F)]. Layering of osteoblasts is a marker of cell differentiation[42] and precedes matrix mineralization. At 4 weeks [Fig. 2(G,H)], the surfaces were fully covered with cells and matrices, and the underlying surface characteristics were not visible. Inability to visualize the underlying substrate surfaces at 4 weeks was probably due to layering of cells, collagen deposition, and mineralization of the matrix. While cell spread happened earlier (up to 24 h) on the rough cpTi surfaces, by 4 weeks, matrix deposition did not appear to be significantly

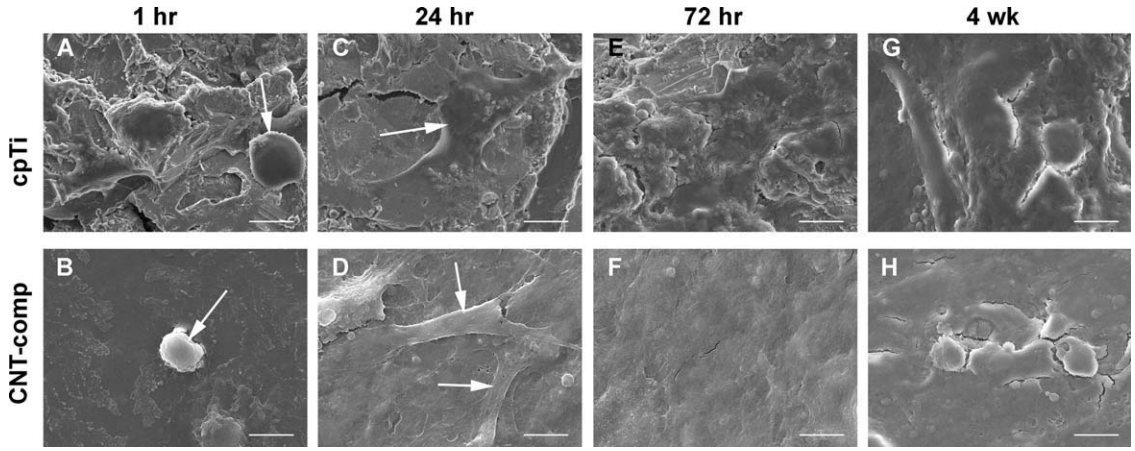

FIGURE 2. Selected scanning electron micrographs of hFOB cultured on cpTi and CNT-comp at different times of culture. Bar = 10 μm. At 1 h, cells (arrows) were round. At 24 h on cpTi, the cells (arrows) were wider than those on CNT. Cells (arrows) on CNT were spindle shaped. The cells had started to form layer. At 72 h, the surfaces were covered with cells, and outlines of the cells are not identifiable. At week 4, all surfaces were covered with cells and matrices. The outlines of cells were not visible.

different between the two surfaces. These results show that both the surfaces were biocompatible at least for 4 weeks.

In addition to studying cellular morphology, we also evaluated cellular proliferation (early response) and differentiation and matrix mineralization (late response) of hFOB cells to the substrates. After 7 days of culture, cell count was significantly higher ($p < 0.05$) on the TC surface compared to CNT-comp or cpTi substrates (Fig. 3). There was no statistical difference in cell proliferation on the CNT-comp compared to cpTi. The better response on TC surface is likely from optimized culture surface for cell growth.

Cellular differentiation was measured by ALP activity, an early differentiation marker.[43] Cells on the TC and CNT-comp surfaces had similar levels of ALP activity, although the cellular proliferation was lower on CNT-comp (Fig. 4). The low cell proliferation but high ALP activity on the CNT-comp suggests that cells started to differentiate earlier on this surface. Despite the highest cell proliferation on TC, differentiation was not equally striking. These *in vitro* results indicate that initial cell proliferation on a surface was not a good indicator of subsequent differentiation.

With increased differentiation, the extracellular matrix of the osteoblasts matures and initiates mineralization. A marker for mineralization is calcium content in the culture. At 4 weeks of culture, matrix calcium content was significantly higher on CNT-comp surface ($p < 0.05$), indicating greatest cell differentiation and maturation (Fig. 5). The TC surface had significantly lower amount of calcium content, compared to both cpTi and CNT-comp, although it had the highest cell proliferation on day 8.

To determine if the calcium to phosphate ratio in the mineralized matrix was similar to that found in bone (i.e., physiologic), and to detect the distribution of cells and calcium in the culture, energy dispersive spectroscopy (EDS) was performed. On surfaces with cells, calcium was detected at peaks of 3.7 and 4 keV and phosphorus was detected at a peak of 2.0 keV (Fig. 6). These peaks were not present on

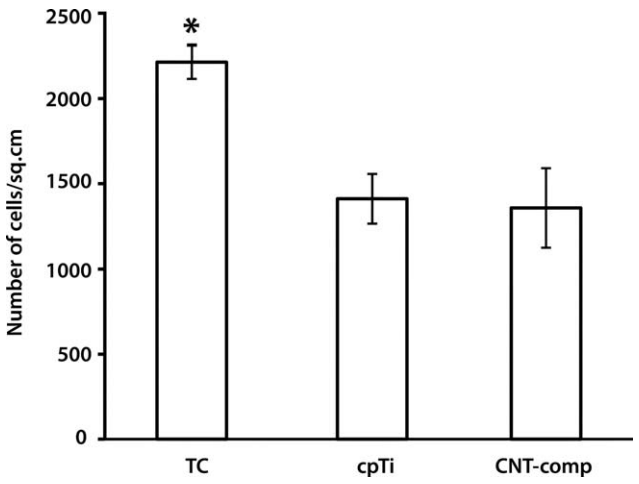

FIGURE 3. Proliferation of hFOB on TC, cpTi and CNT-comp ($n = 6$) at day 7 of culture. Cells were plated at a density of 50,000 cells/well on the substrates in six-well dishes. On day 7, cells grown on the substrates were trypsinized and counted in a Coulter counter. Error bars= SEM, (*$p < 0.05$).

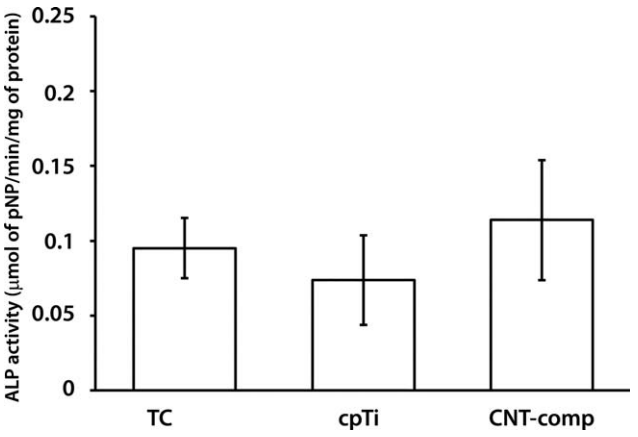

FIGURE 4. Normalized ALP activity of hFOB cultured on TC, cpTi, and CNT-comp on day 7. Cells on CNT-comp surface had highest ALP activity, indicating increased cellular differentiation. Error bars = SEM.

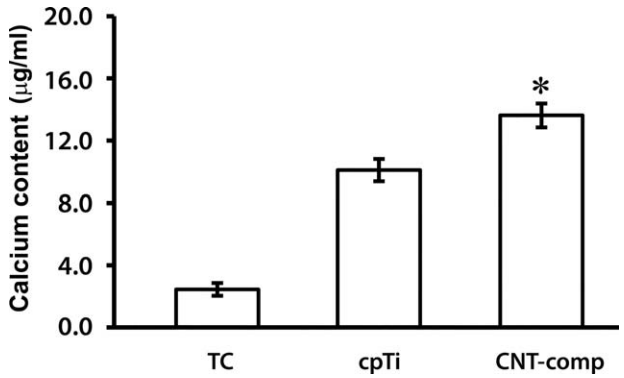

FIGURE 5. Calcium content at week 4 in cultures of hFOB on TC, cpTi, and CNT-comp. Calcium was extracted from the culture and measured colorimetrically. Error bars = SEM, (*$p < 0.05$).

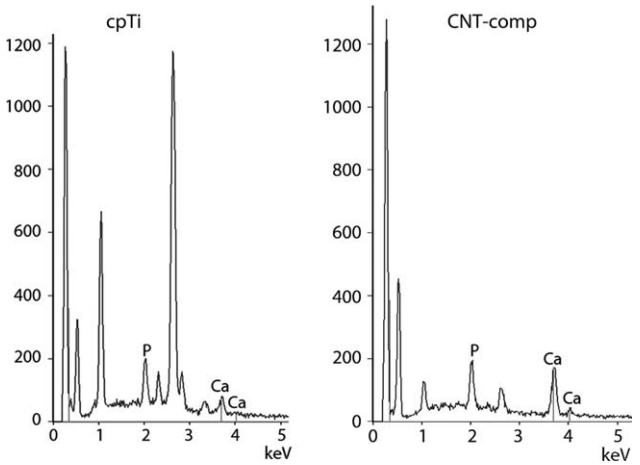

FIGURE 6. Electron dispersive spectroscopy (EDS) of substrates with cells 4 weeks after cell plating. On cell-free surfaces, Ca and P had no detectable peaks (data not shown). After culture, both cpTi and CNT-comp surfaces showed prominent peaks of Ca and P. The area under the peak was measured by SigmaScan Pro.

surfaces without cells (data not shown). Using SigmaScan Pro software (SPSS Science, Chicago, IL), we measured the areas under the peaks of phosphorus and calcium. The ratio of the areas of the calcium to phosphate peaks from the CNT-comp samples was 3:2 (1.5), which is close to the theoretical ratio of calcium to phosphate [$Ca_{10}(PO_4)_6(OH)_2$, Ca/P ratio = 1.67] in bone. On cpTi, the ratio was lower (1.33) suggesting, the calcium phosphate crystals formed on cpTi were not similar to those formed in bone.

The distribution of calcium on the surfaces of the substrates was also examined using EDS. In Figure 7, the dots represent locations of calcium crystals and the number of dots were counted using Adobe Photoshop CS4 (Adobe Systems Inc, San Jose, CA). The number of calcium crystals on CNT-comp (3993 ± 17) was significantly higher ($p < 0.05$) than on cpTi (3165 ± 26). This finding was consistent with the biochemical assays that showed cpTi had the lowest amount of calcium deposition.

Although our *in vitro* studies provided promising results for CNT-comps, the *in vivo* effects of CNTs in bone are not clearly known. To our knowledge, two publications have reported the effects of implanted CNTs in bone.[29,30] Both the reports evaluated healing of noncritical sized defects. A critical sized defect would not completely close the defect with bone without addition of scaffold. We, therefore, examined the biocompatibility of these materials in a critically sized defect in the calvaria of 6-week-old rats ($n = 3$ per material). Six weeks after the implantation, histomorphometric analysis revealed that bony extensions formed in close approximation to the CNT-comp [Fig. 8(A)]. Furthermore, there were no histological signs of inflammation or rejection of the grafted CNT-comps. Several areas of the CNT-comp were covered only with fibrous tissues. The control animals, without any graft, did not show similar bony extensions [Fig. 8(B)]. Examination under polarized light [Fig. 8(C)] revealed patterns of collagen deposition and bone formation.[44] In addition, a fibrous tissue formed in close contact with the CNT-comp surface.

DISCUSSION

In this study, a composite of chemically functionalized single-walled carbon nanotube with polymers using a layer-by-

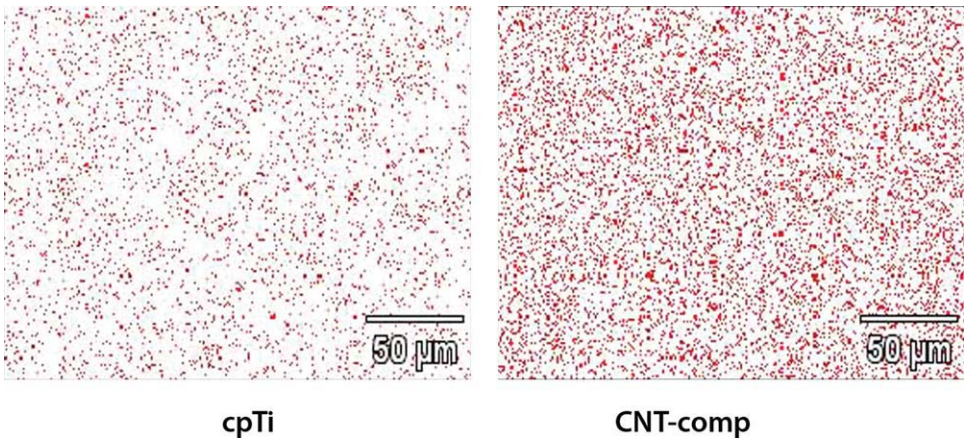

FIGURE 7. Surface calcium mapping using EDS on substrates with cells 4 weeks after cell plating. The red dots indicate locations of calcium. All the three substrates showed uniform distribution of calcium, while CNT-comp had higher amount of calcium compared to cpTi ($p < 0.05$). [Color figure can be viewed in the online issue, which is available at wileyonlinelibrary.com.]

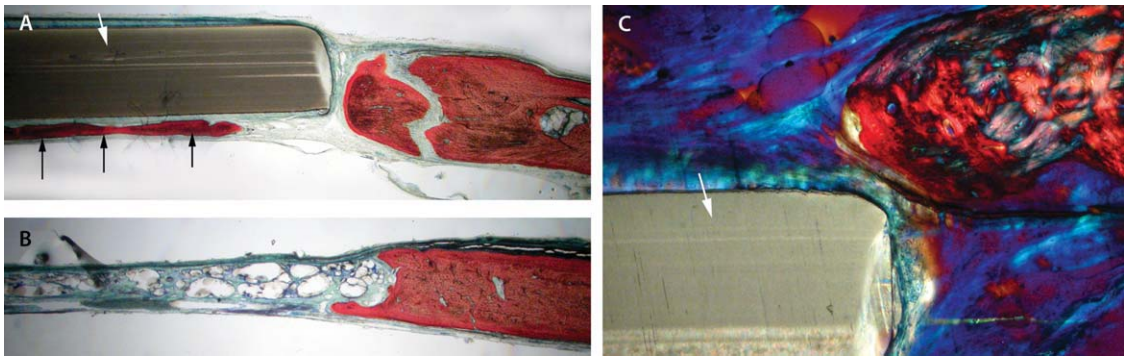

FIGURE 8. Histological sections through the cranium containing CNT-comp disks (A and C), and no substrate (B). (A) Shows an extension of bone (black arrows) on one side of the CNT-comp disk (white arrow). A thin layer of fibrous tissue was present between the bone and the disk. There is no contact visible between the new linear bone and the edge of surgical defect. (B) Shows a cross section through a control animal without any substrate. No new bone formation is seen in the defect. Only small projections of the osseous structures were visible at the margins of the defects. The defect was closed with fibrous tissue only. (C) is a polarized view of a histological section through a CNT-comp and the cranial bone. The bone adjacent to the disk is mature lamellar type, while the remaining bone is immature or irregular woven bone. [Color figure can be viewed in the online issue, which is available at wileyonlinelibrary.com.]

layer technique was fabricated. This CNT composite had physical properties within the range of cortical and trabecular bone. The CNT-comp was not toxic to the cells (*in vitro*) or tissues (*in vivo*). During cell culture, both CNT-comp and cpTi surfaces were covered by cells. However, calcium deposition on the CNT-comp was higher than on the cpTi. These results suggest that osteoblasts will proliferate and differentiate on CNT comp surface as well as or better than cpTi. *In vivo* studies showed adequate bone formation around non-porous CNT-composite. Bone formation may be improved if the CNT-comp was porous to allow better transport of nutrients.

A composite of CNT with polymers can be created in several ways.[45,46] However, CNT-comps assembled using layer-by-layer technique have been shown to provide better mechanical properties than those fabricated with traditional methods.[4] We used PDDA, PEI, and PSS for the layer-by-layer assembly because of their charge densities and biocompatibility. In our fabrication method, the CNTs were coated with a thin layer of PEI ($\sim$4 nm), leaving parts of the SWCNTs exposed to the cellular environment. Therefore, the response of osteoblasts, as observed in our study, can be attributed to CNT as well as polymers. Several researchers[36,37,39,40] have reported that the lower bound of modulus of trabecular and cortical bone to be of the same order of magnitude as that obtained in this study. By changing the number of CNT layers the mechanical properties can be varied. It is therefore possible to create a scaffold with similar mechanical properties as bone for specific anatomic locations.

Several studies had reported that CNTs can be toxic to some types of cells.[7,10,47,48] Our several unpublished work showed CNT being nontoxic. A hemolytic assay was conducted by incubating CNT-comp in oxalated rabbit blood. After 1 h of incubation, the percent hemolyis was similar to positive (0.1% sodium carbonate) and negative controls (normal saline without CNT-comp). In an agar overlay assay, mouse embryo fibroblast cells (clone L-929) were coated with agar. CNT-comp samples were placed directly on the solidified agar overlay testing surfaces. Control surfaces were latex and polypropylene. Following 24–36 h of incubation, cells were evaluated microscopically for morphology. This experiment also showed the effect of CNT-comp being similar to the control surface. An MTT assay was conducted using SWCNT particles in a culture of hFOB cells. In this assay, the functionalized SWCNTs did not appear to be toxic.

The proliferation of hFOB cells on the CNT-comp indicated that this substrate was not toxic to the cells. Other investigators have shown high cell proliferation on CNTs, particularly on single-walled tubes.[18,49,50] We compared the cell proliferation on CNT-comp to those on TC and cpTi. The high number of cells on TC surfaces can be attributed to the surface of the culture dishes having been optimized for cell growth. The cpTi surface was rougher than CNT-comp. Rough surfaces are known to promote cell proliferation compared to smooth surface.[41]

The early spread of cells is an indicator of initial biocompatibility, but it may not predict future differentiation of the cells. The hFOB cells were slow to spread on CNT-comp compared to cpTi, but were able to differentiate on these surfaces at day 7 and week 4 of culture. Previous work indicated that cell spread requires 6–8 h on smooth surfaces.[41] In that study, it was shown that the cells spread wider and earlier on rough surfaces compared to smooth surfaces.

After the cells spread on a surface, they assemble as layers forming a nodule. The nodule is the center of initiation of mineralization. A round cell thus is not at a stage of maturity or initiation of mineralization. Some reports have misinterpreted round cell on MWCNT surface on day 5 of culture as a mature osteocyte.[18] It is highly unlikely that the cells differentiated in 3 or 5 days into osteocytes. In addition, it was claimed that the cells were embedded in bone matrix. When cells become embedded in extracellular matrix, the outlines of the cells are difficult to identify, as shown in our SEM images of 72 h and 4 weeks. A persistently round cell indicates that the host surface is not conducive for cell spreading. In the same study, cells did spread on both SWCNTs and on control glass surfaces. In another

study using MWCNTs coated with HA, hFOB cells were claimed to differentiate to maturity on day 3.[22] A maturity by day 3 is unlikely as cells continue to proliferate for several days after plating.

Although the cellular proliferation was lower on CNT-comp, ALP activity of osteoblast cultured on CNT-comp was similar to that on cpTi. The low cell proliferation and high ALP activity on the CNT-comp suggest that cells started to differentiate earlier on this surface. The TC, which had highest cell proliferation, had low ALP activity. These *in vitro* results indicate that initial cell proliferation on a surface was not a good indicator of subsequent differentiation.

Matrix mineralization was measured in two ways: total calcium was measured biochemically, and surface calcium was measured using EDS. The biochemical assays showed significantly higher calcium deposition on CNT-comp compared to the other substrates. EDS studies also confirmed that surface calcium was highest on CNT-comp.

In our study, we created a critical sized defect to evaluate the capacity of the CNT-comp to promote bone healing. Bone formation was on only one side of the CNT-comp. In addition, a fibrous tissue formed in close contact with the CNT-comp surface. In some histological sections (data not shown), bone started forming from the edge of the defect towards the center of the CNT-comp disk, while other sections showed bone formation without connection to the edge of the defect. The apparently isolated bone was likely connected to the edge of the defect but appeared isolated due to orientation of the tissue slices and thus does not indicate heterotopic ossification. Although both the surfaces of the CNT-comp disks were identically prepared, the nonporous nature of the CNT-comp disks may have restricted the flow of nutrients and endogenous bone stimulating factors, thus promoting bone formation only on the inner side. In all the cases, the bone did not completely close the critical defect at 6 weeks after implantation. This may be due to the relatively short period of healing. CNT-comp disks were coated with polymer and have roughness only on the nanoscale. Rough surfaces induce better bone formation.[51,52] Therefore, bone formation on CNT-comp may improve with increased surface roughness. On polarized views, the presence of lamellar bone near the CNT-comp disk indicated physiologic bone repair to heal the surgical defect.

CONCLUSION

CNT-composites have been developed to meet the mechanical properties of bone, specifically the modulus of elasticity. Our results show that early *in vitro* response of cells (i.e., cell proliferation) may not be a good indicator of future success of biomaterials. Cell proliferation was highest on the TC surface, but differentiation and matrix mineralization was low. CNT-comp allowed better mineral formation compared to the TC or cpTi substrates. The EDS study confirmed that the surface of CNT-comp was better in promoting matrix mineralization than cpTi surface. As the CNT-comp was compatible to cells, a porous or rough CNT-comp disk may encourage even better cell proliferation and matrix mineralization. *In vivo* studies showed that CNT-comp was biocompatible and promoted bone formation. Thus, CNT-composites may be promising materials for use in dental implants and for repair of bone defects.

ACKNOWLEDGMENTS

Partial funding for this research was provided by the University of Minnesota Grant-in-aid of research. Parts of this work were carried out in the University of Minnesota Nanofabrication Center which receives partial support from NSF through the NNIN program.

REFERENCES

1. Sinha N, Yeow JT. Carbon nanotubes for biomedical applications. IEEE Trans Nanobioscience 2005;4:180–195.
2. Bassett CA. Fundamental and practical aspects of therapeutic uses of pulsed electromagnetic fields (PEMFs). Crit Rev Biomed Eng 1989;17:451–529.
3. Supronowicz PR, Ajayan PM, Ullmann KR, Arulanandam BP, Metzger DW, Bizios R. Novel current-conducting composite substrates for exposing osteoblasts to alternating current stimulation. J Biomed Mater Res 2002;59:499–506.
4. Mamedov AA, Kotov NA, Prato M, Guldi DM, Wicksted JP, Hirsch A. Molecular design of strong single-wall carbon nanotube/polyelectrolyte multilayer composites. Nat Mater 2002;1:190–194.
5. Olek M, Ostrander J, Jurga S, Mohwald H, Kotov NA, Kempa K, Giersig M. Layer-by-layer assembled composites from multiwall carbon nanotubes with different morphologies. Nano Lett 2004;4: 1889–1895.
6. Sayes CM, Liang F, Hudson JL, Mendez J, Guo W, Beach JM, Moore VC, Doyle CD, West JL, Billups WE, Ausman KD, Colvin VL. Functionalization density dependence of single-walled carbon nanotubes cytotoxicity in vitro. Toxicol Lett 2006;161:135–142.
7. Shvedova AA, Castranova V, Kisin ER, Schwegler-Berry D, Murray AR, Gandelsman VZ, Maynard A, Baron P. Exposure to carbon nanotube material: Assessment of nanotube cytotoxicity using human keratinocyte cells. J Toxicol Environ Health A 2003;66: 1909–1926.
8. Lam CW, James JT, McCluskey R, Arepalli S, Hunter RL. A review of carbon nanotube toxicity and assessment of potential occupational and environmental health risks. Crit Rev Toxicol 2006;36: 189–217.
9. Nimmagadda A, Thurston K, Nollert MU, McFetridge PS. Chemical modification of SWNT alters in vitro cell-SWNT interactions. J Biomed Mater Res A 2006;76:614–625.
10. Cui D, Tian F, Ozkan CS, Wang M, Gao H. Effect of single wall carbon nanotubes on human HEK293 cells. Toxicol Lett 2005;155: 73–85.
11. Monteiro-Riviere NA, Nemanich RJ, Inman AO, Wang YY, Riviere JE. Multi-walled carbon nanotube interactions with human epidermal keratinocytes. Toxicol Lett 2005;155:377–384.
12. Shvedova AA, Kisin E, Murray AR, Johnson VJ, Gorelik O, Arepalli S, Hubbs AF, Mercer RR, Keohavong P, Sussman N, Jin J, Yin J, Stone S, Chen BT, Deye G, Maynard A, Castranova V, Baron PA, Kagan VE. Inhalation vs. aspiration of single-walled carbon nanotubes in C57BL/6 mice: Inflammation, fibrosis, oxidative stress, and mutagenesis. Am J Physiol Lung Cell Mol Physiol 2008;295:L552–L565.
13. Warheit DB, Laurence BR, Reed KL, Roach DH, Reynolds GA, Webb TR. Comparative pulmonary toxicity assessment of single-wall carbon nanotubes in rats. Toxicol Sci 2004;77:117–125.
14. Garibaldi S, Brunelli C, Bavastrello V, Giorgio Ghigliotti G, Nicolini C. Carbon nanotube biocompatibility with cardiac muscle cells. Nanotech 2006;17:391–397.
15. Smart SK, Cassady AI, Lu GQ, Martin DJ. The biocompatibility of carbon nanotubes. Carbon 2006;44:1034–1047.
16. Ni Y, Hu H, Malarkey EB, Zhao B, Montana V, Haddon RC, Parpura V. Chemically functionalized water soluble single-walled carbon nanotubes modulate neurite outgrowth. J Nanosci Nanotechnol 2005;5:1707–1712.

17. McKenzie JL, Waid MC, Shi R, Webster TJ. Decreased functions of astrocytes on carbon nanofiber materials. Biomaterials 2004;25: 1309–1317.
18. Zanello LP, Zhao B, Hu H, Haddon RC. Bone cell proliferation on carbon nanotubes. Nano Lett 2006;6:562–567.
19. Verdejo R, Jell G, Safinia L, Bismarck A, Stevens MM, Shaffer MS. Reactive polyurethane carbon nanotube foams and their interactions with osteoblasts. J Biomed Mater Res A 2009;88: 65–73.
20. Wang W, Watari F, Omori M, Liao S, Zhu Y, Yokoyama A, Uo M, Kimura H, Ohkubo A. Mechanical properties and biological behavior of carbon nanotube/polycarbosilane composites for implant materials. J Biomed Mater Res B Appl Biomater 2007;82: 223–230.
21. Eliason MT, Sunden EO, Cannon AH, Graham S, Garcia AJ, King WP. Polymer cell culture substrates with micropatterned carbon nanotubes. J Biomed Mater Res A 2008;86:996–1001.
22. Balani K, Anderson R, Laha T, Andara M, Tercero J, Crumpler E, Agarwal A. Plasma-sprayed carbon nanotube reinforced hydroxyapatite coatings and their interaction with human osteoblasts in vitro. Biomaterials 2007;28:618–624.
23. MacDonald RA, Laurenzi BF, Viswanathan G, Ajayan PM, Stegemann JP. Collagen-carbon nanotube composite materials as scaffolds in tissue engineering. J Biomed Mater Res A 2005;74:489–496.
24. Shokuhfar T, Makradi A, Titus E, Cabral G, Ahzi S, Sousa AC, Belouettar S, Gracio J. Prediction of the mechanical properties of hydroxyapatite/polymethyl methacrylate/carbon nanotubes nanocomposite. J Nanosci Nanotechnol 2008;8:4279–4284.
25. Weisenberger MC, Grulke EA, Jacques D, Rantell T, Andrews R. Enhanced mechanical properties of polyacrylonitrile/multiwall carbon nanotube composite fibers. J Nanosci Nanotechnol 2003;3: 535–539.
26. Glassman AH, Bobyn JD, Tanzer M. New femoral designs: Do they influence stress shielding? Clin Orthop Relat Res 2006;453: 64–74.
27. Whiteside LA. The effect of stem fit on bone hypertrophy and pain relief in cementless total hip arthroplasty. Clin Orthop Relat Res 1989;247:138–147.
28. Stoppie N, Van Oosterwyck H, Jansen J, Wolke J, Wevers M, Naert I. The influence of Young's modulus of loaded implants on bone remodeling: An experimental and numerical study in the goat knee. J Biomed Mater Res A 2009;90:792–803.
29. Usui Y, Aoki K, Narita N, Murakami N, Nakamura I, Nakamura K, Ishigaki N, Yamazaki H, Horiuchi H, Kato H, Taruta S, Kim YA, Endo M, Saito N. Carbon nanotubes with high bone-tissue compatibility and bone-formation acceleration effects. Small 2008;4: 240–246.
30. Sitharaman B, Shi X, Walboomers XF, Liao H, Cuijpers V, Wilson LJ, Mikos AG, Jansen JA. In vivo biocompatibility of ultra-short single-walled carbon nanotube/biodegradable polymer nanocomposites for bone tissue engineering. Bone 2008;43:362–370.
31. Oliver WC, Pharr GM. An improved technique for determining hardness and elastic modulus using load and displacement sensing indentation experiments. J Mater Res 1992;7:1564–1583.
32. Harris SA, Enger RJ, Riggs BL, Spelsberg TC. Development and characterization of a conditionally immortalized human fetal osteoblastic cell line. J Bone Miner Res 1995;10:178–186.
33. Nussenbaum B, Rutherford RB, Krebsbach PH. Bone regeneration in cranial defects previously treated with radiation. Laryngoscope 2005;115:1170–1177.
34. Donath K, Breuner G. A method for the study of undecalcified bones and teeth with attached soft tissues. The Sage-Schliff (sawing and grinding) technique. J Oral Pathol 1982;11:318–326.
35. Thompson DM, Rohrer MD, Prasad HS. Comparison of bone grafting materials in human extraction sockets: Clinical, histologic, and histomorphometric evaluations. Implant Dent 2006;15:89–96.
36. Xu J, Rho JY, Mishra SR, Fan Z. Atomic force microscopy and nanoindentation characterization of human lamellar bone prepared by microtome sectioning and mechanical polishing technique. J Biomed Mater Res A 2003;67:719–726.
37. Lee FY, Rho JY, Harten R Jr, Parsons JR, Behrens FF. Micromechanical properties of epiphyseal trabecular bone and primary spongiosa around the physis: An in situ nanoindentation study. J Pediatr Orthop 1998;18:582–585.
38. Tang Z, Kotov NA, Magonov S, Ozturk B. Nanostructured artificial nacre. Nat Mater 2003;2:413–418.
39. Nomura T, Katz JL, Powers MP, Saito C. Evaluation of the micromechanical elastic properties of potential bone-grafting materials. J Biomed Mater Res B Appl Biomater 2005;73:29–34.
40. Hengsberger S, Kulik A, Zysset P. A combined atomic force microscopy and nanoindentation technique to investigate the elastic properties of bone structural units. Eur Cell Mater 2001;1:12–17.
41. Ahmad M, Gawronski D, Blum J, Goldberg J, Gronowicz G. Differential response of human osteoblast-like cells to commercially pure (cp) titanium grades 1 and 4. J Biomed Mater Res 1999;46: 121–131.
42. Bhargava U, Bar-Lev M, Bellows C, Aubin J. Ultrastructural analysis of bone nodules formed in vitro by isolated fetal rat calvarial cells. Bone 1988;9:155–163.
43. Stein G, Lian J, Owen T. Relationship of cell growth to the regulation of tissue-specific gene expression during osteoblast differentiation. FASEB J 1990;4:3111–3123.
44. Clineff TD, Erbe EM, Bauer TW, Carroll BE. Analytical technique for quantification of selected resorbable calcium phosphate bone void fillers with the use of polarized-light microscopy. J Biomed Mater Res B Appl Biomater 2005;72:125–130.
45. Thostensen ET, Chou TW. Aligned multi-walled carbon nanotube-reinforced composite: Processing and mechanical characterization. J Phys D: Appl Phys. 2002;35:L77–L80.
46. Thostensen ET, Ren Z, Chou TW. Advances in science and technology of carbon nanotubes and their composite: A review. Comp Sci Tech 2001;61:1899–1912.
47. Manna SK, Sarkar S, Barr J, Wise K, Barrera EV, Jejelowo O, Rice-Ficht AC, Ramesh GT. Single-walled carbon nanotube induces oxidative stress and activates nuclear transcription factor-kappaB in human keratinocytes. Nano Lett 2005;5:1676–1684.
48. Ding L, Stilwell J, Zhang T, Elboudwarej O, Jiang H, Selegue JP, Cooke PA, Gray JW, Chen FF. Molecular characterization of the cytotoxic mechanism of multiwall carbon nanotubes and nano-onions on human skin fibroblast. Nano Lett 2005;5:2448–2464.
49. Aoki N, Akasaka T, Watari F, Yokoyama A. Carbon nanotubes as scaffolds for cell culture and effect on cellular functions. Dent Mater J 2007;26:178–185.
50. Li X, Gao H, Uo M, Sato Y, Akasaka T, Feng Q, Cui F, Liu X, Watari F. Effect of carbon nanotubes on cellular functions in vitro. J Biomed Mater Res A 2009;91:132–139.
51. Schwarz ML, Kowarsch M, Rose S, Becker K, Lenz T, Jani L. Effect of surface roughness, porosity, and a resorbable calcium phosphate coating on osseointegration of titanium in a minipig model. J Biomed Mater Res A 2009;89:667–678.
52. Shalabi MM, Gortemaker A, Van't Hof MA, Jansen JA, Creugers NH. Implant surface roughness and bone healing: A systematic review. J Dent Res 2006;85:496–500.